VLSI Design
1995, Vol. 3, No. 2, pp. 201–210
Reprints available directly from the publisher
Photocopying permitted by license only

© 1995 OPA (Overseas Publishers Association)
Amsterdam B.V. Published under license by
Gordon and Breach Science Publishers SA
Printed in Malaysia

Resonant Tunneling in the Quantum Hydrodynamic Model

CARL L. GARDNER*
Department of Computer Science and Department of Mathematics, Duke University,
Durham, NC 27708-0129

(Received December 1, 1993)

The phenomenon of resonant tunneling is simulated and analyzed in the quantum hydrodynamic (QHD) model for semiconductor devices. Simulations of a parabolic well resonant tunneling diode at 77 K are presented which show multiple regions of negative differential resistance (NDR) in the current-voltage curve. These are the first simulations of the QHD equations to show multiple regions of NDR.

Resonant tunneling (and NDR) depend on the quantum interference of electron wavefunctions and therefore on the phases of the wavefunctions. An analysis of the QHD equations using a moment expansion of the Wigner-Boltzmann equation indicates how phase information is retained in the hydrodynamic equations.

Key Words: *quantum hydrodynamic model, resonant tunneling diode.*

1. INTRODUCTION

Resonant tunneling of electrons in quantum semiconductor devices can be modeled by adding quantum corrections to the classical hydrodynamic equations. The leading $O(\hbar^2)$ quantum corrections include the effects of particle tunneling through potential barriers and particle buildup in potential wells.

I will present simulations of a GaAs/$Al_XGa_{1-X}As$ parabolic well resonant tunneling diode at 77 K using the quantum hydrodynamic (QHD) equations. The QHD simulations show multiple regions of negative differential resistance (NDR) in the current-voltage curve. These are the first simulations of the QHD equations to show multiple regions of NDR.

Resonances in the current-voltage curve of the resonant tunneling diode occur as electrons tunnel coherently or sequentially through the double barriers. Sequential tunneling occurs if electrons tunnel through the first barrier, undergo scattering, and then tunnel through the second barrier. Coherent tunneling may be interpreted as the constructive interference of multiply reflected electron waves within the well. Resonant tunneling in actual devices usually involves a mixture of coherent and sequential tunneling. Scattering broadens the resonances and reduces the peak to valley ratios in the current-voltage curve. In this investigation, I will present two sets of simulations of the resonant tunneling diode: in the first set, scattering takes place throughout the device, while in the second set the collision terms in the QHD model are set to zero in the barriers and the well, to insure that the electron tunneling is coherent.

Coherent resonant tunneling and negative differential resistance depend on the quantum interference of electron wavefunctions, and therefore on the phases of the wavefunctions. I will indicate how phase information is retained in the hydrodynamic equations through an analysis of the QHD equations using a moment expansion of the Wigner-Boltzmann equation.

*Research supported in part by the U.S. Army Research Office under grant DAAL03-91-G-0146 and by the National Science Foundation under grant DMS-9204189.

2. THE QUANTUM HYDRODYNAMIC MODEL

The QHD equations have the same structure [1] as the classical hydrodynamic equations:

$$\frac{\partial n}{\partial t} + \frac{1}{m}\frac{\partial \Pi_i}{\partial x_i} = 0 \tag{1}$$

$$\frac{\partial \Pi_j}{\partial t} + \frac{\partial}{\partial x_i}(u_i \Pi_j - P_{ij}) = -n\frac{\partial V}{\partial x_j} - \frac{\Pi_j}{\tau_p} \tag{2}$$

$$\frac{\partial W}{\partial t} + \frac{\partial}{\partial x_i}(u_i W - u_j P_{ij} + q_i) = -\frac{\Pi_i}{m}\frac{\partial V}{\partial x_i} - \frac{(W - \frac{3}{2}nT_0)}{\tau_w} \tag{3}$$

$$\nabla \cdot (\varepsilon \nabla V) = e^2(N_D - N_A - n) \tag{4}$$

where n is the electron density, m is the effective electron mass, Π_i is the momentum density, $\mathbf{u}$ is the velocity, P_{ij} is the stress tensor, $V = -e\phi$ is the potential energy, ϕ is the electric potential, $e > 0$ is the electronic charge, W is the energy density, $\mathbf{q}$ is the heat flux, T_0 is the temperature of the semiconductor lattice in energy units (k_B is set equal to 1), ε is the dielectric constant, N_D is the density of donors, and N_A is the density of acceptors. Spatial indices i, j equal 1, 2, 3, and repeated indices are summed over. Eq. (1) expresses conservation of electron number, Eq. (2) expresses conservation of momentum, Eq. (3) expresses conservation of energy, and Eq. (4) is Poisson's equation. The classical collision terms in Eqs. (2) and (3) are modeled by the relaxation time approximation, with momentum and energy relaxation times τ_p and τ_w. The heat flux is specified here by Fourier's law $\mathbf{q} = -\kappa \nabla T$, where T is the electron temperature.

The quantum corrections to the classical hydrodynamic equations appear in the stress tensor and the energy density. As $\hbar \to 0$, the quantum corrections can be developed in a power series in $\hbar^2$. The actual expansion parameter is $\hbar^2/8mTl^2$, where l is a characteristic length scale of the problem [2, 3]. For the resonant tunneling diode in section 3 with $T \approx T_0 = 77$ K and $l = 100$ Å, the expansion parameter ≈ 0.23.

In Ref. [1], I showed that for the $O(\hbar^2)$ momentum-shifted thermal equilibrium Wigner distribution function, the momentum density is given by

$$\Pi_i = mnu_i \tag{5}$$

the stress tensor by

$$P_{ij} = -nT\delta_{ij} + \frac{\hbar^2 n}{12m}\frac{\partial^2}{\partial x_i \partial x_j}\log(n) + O(\hbar^4) \tag{6}$$

and the energy density by

$$W = \frac{3}{2}nT + \frac{1}{2}mnu^2 - \frac{\hbar^2 n}{24m}\nabla^2 \log(n) + O(\hbar^4). \tag{7}$$

Wigner [4] derived the quantum correction to the energy density (in a different form). Ancona and Tiersten [5] proposed the quantum correction to the stress tensor on general thermodynamical grounds, and Ancona and Iafrate [2] later derived the correction in the Wigner formalism. A one-dimensional version of the QHD equations was derived by Grubin and Kreskovsky in Ref. [6].

3. SIMULATIONS OF MULTIPLE RESONANCES

I will simulate a GaAs resonant tunneling diode with double $Al_{0.8}Ga_{0.2}As$ barriers and a parabolic $Al_XGa_{1-X}As$ quantum well. The diode consists of an n^+ source (at the left), an n channel, and an n^+ drain (at the right). The doping density $N_D = 10^{18}$ cm^{-3} in the n^+ source and drain, and $N_D = 5 \times 10^{15}$ cm^{-3} in the n channel (see Figure 1). The channel is 500 Å long, the barriers are 30 Å wide, and the well between the barriers is 300 Å wide. The device has 70 Å spacers between the barriers and the contacts (source and drain) to enhance NDR. The barrier height $\mathscr{B}$ is set equal to 0.7 eV. In the well, the Al mole fraction X varies between 0.8 and 0, so that the potential barrier height in the well is (see Figure 2)

$$\mathscr{B}_{well} = 0.7\,eV\left[\frac{x - \frac{1}{2}(x_L + x_R)}{\frac{1}{2}(x_R - x_L)}\right]^2 \tag{8}$$

where x_L and x_R are the coordinates of the left and right edges of the well. The left edge of the first barrier and the right edge of the second barrier are modeled as step functions. (Computationally the step function goes from 0 to 1 over one Δx.)

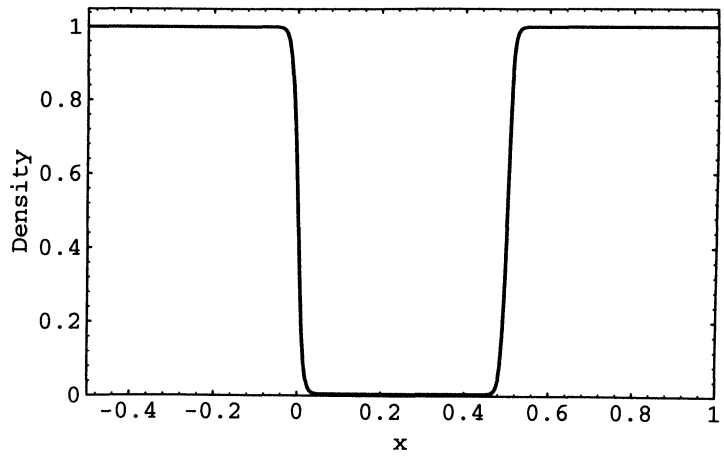

FIGURE 1 Doping/10^{18} cm^{-3}.

For the classical momentum and energy relaxation times, I use modified Baccarani-Wordemann models:

$$\tau_p = \tau_{p0}\frac{T_0}{T} \tag{9}$$

$$\tau_w = \frac{\tau_p}{2}\left(1 + \frac{\frac{3}{2}T}{\frac{1}{2}mv_s^2}\right) \tag{10}$$

where the low-energy momentum relaxation time τ_{p0} is set equal to 0.9 picoseconds from the low-field electron mobility in GaAs at 77 K. For lower valley electrons in GaAs at 77 K, the effective electron mass $m = 0.063\ m_e$, where m_e is the electron mass, and the saturation velocity $v_s \approx 2 \times 10^7$ cm/s. I set $\kappa_0 = 0.4$ in the Wiedemann-Franz formula for thermal conductivity

$$\mathbf{q} = -\kappa\nabla T,\ \kappa = \kappa_0\tau_{p0}nT_0/m. \tag{11}$$

The dielectric constant $\varepsilon = 12.9$ for GaAs.

I discretize the 1D steady-state QHD equations using the second upwind method and compute the solution using a damped Newton method (see Ref. [1] for details). The barrier height $\mathscr{B}$ is incorporated into the QHD transport equations (1)–(3) by replacing $V \to V + \mathscr{B}$. Poisson's equation is not changed.

The current voltage curve for the resonant tunneling diode at 77 K is plotted in Figure 3, using a grid

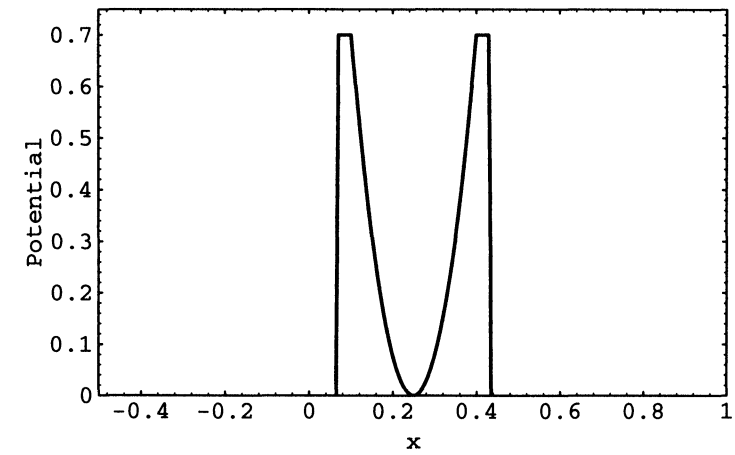

FIGURE 2 Barrier and well heights in eV.

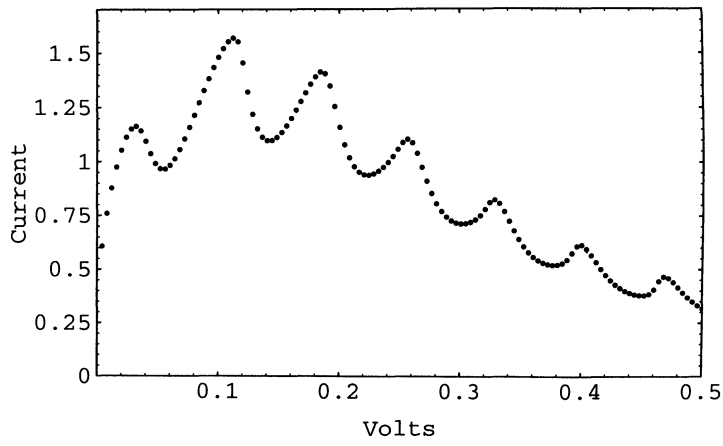

FIGURE 3 Current density in milliamps/cm^2 vs. voltage for the resonant tunneling diode at 77 K with scattering throughout the device. The dots represent computed solution points.

with 300 Δx. For these simulations, scattering takes place throughout the device. There are seven resonances and seven regions of negative differential resistance in the current-voltage curve between 0 and 0.5 volts.

Figure 4 presents the current-voltage curve for the same device with the classical collision terms in the momentum and energy equations (2) and (3) turned off in the barriers and the well. Electron tunneling in this case must be purely coherent rather than sequential plus coherent, since there is no scattering in the well or barriers. There are twelve resonances and seven regions of negative differential resistance in the current-voltage curve between 0 and 1 volt.

Note that there are five resonant "shoulders" in the current-voltage curve between 0 and 0.33 volts, and that the sixth through twelfth resonances become more pronounced as V increases. Ref. [7] explains this effect, which was observed in an experimental device: Below 0.33 volts, electrons tunnel out of the well through the thick portion of the parabolic well in Figure 2, and the transmission resonance widths are small. As the voltage bias increases above 0.33 volts, the transmission resonance widths rapidly increase because (i) the right barrier height is progressively reduced and (ii) electrons tunnel out of the well through the thin portion of the parabolic well.

The resonant peaks of the current-voltage curve occur as the electrons tunneling through the first barrier come into resonance with the energy levels of the quantum well. The locations of the resonances can be qualitatively understood from the

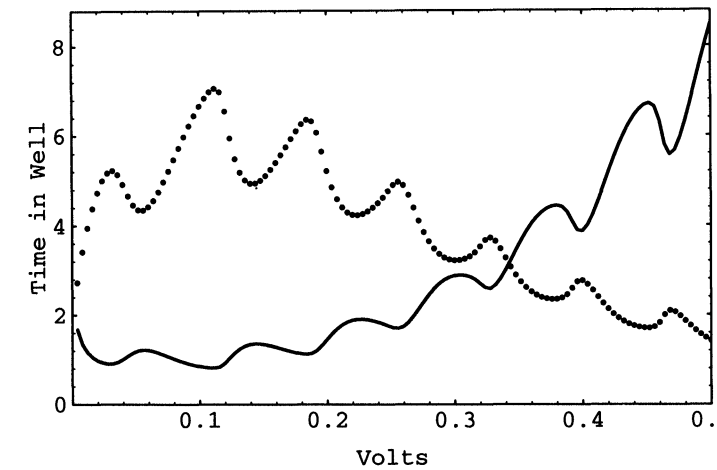

FIGURE 4 Current density in milliamps/cm^2 vs. voltage for the resonant tunneling diode at 77 K with scattering turned off in the barriers and the well. The dots represent computed solution points.

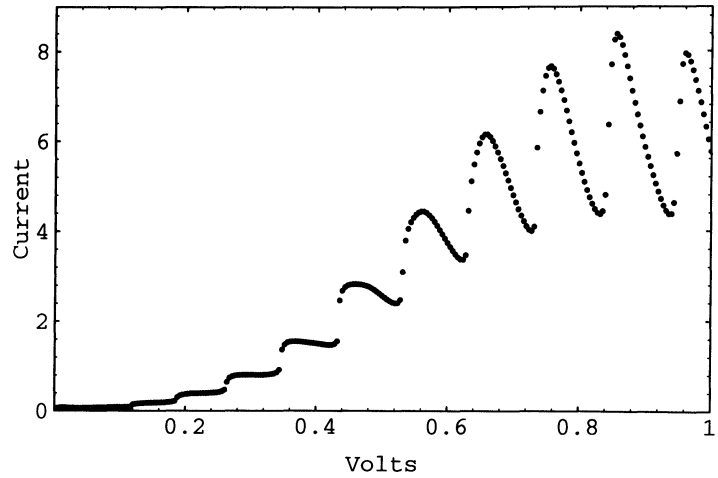

FIGURE 5 Time (solid line) in 10^{-4} seconds spent by electrons in the well vs. voltage with scattering throughout the device. For reference, a scaled version of the current density (dots) is also shown.

energy levels of an infinite parabolic well. For an infinite well,

$$E_\lambda = \left(\lambda + \frac{1}{2}\right)\hbar\sqrt{\frac{8\mathscr{B}}{mx_0^2}} \approx \left(\lambda + \frac{1}{2}\right)0.087\ \text{eV} \quad (12)$$

where $x_0 = 300$ Å is the width of the finite well and λ is a non-negative integer. The energy levels of the infinite parabolic well are linearly spaced in λ with a spacing of 87 meV, compared with the linear spacings of approximately 70 mV (with scattering throughout the device) and 100 mV (with scattering turned off in the barriers and the well) for the computed peaks in the current-voltage curves. The first peak with scattering throughout the device occurs at 0.030 volts, compared with $E_0 \approx 0.044$ eV.

The overall shape of the current-voltage curve in Figure 3—the rise to a peak at 0.11 volts and the fall to the valley at 0.58—is determined by the negative differential resistance of a 0.7 eV high double barrier square well with an effective width of approximately 75 Å. The energy levels of the parabolic well modulate this basic shape.

The time spent by electronics in the well is shown in Figure 5. The "dwell" time has relative maxima at voltages corresponding to valleys (relative minima) of the current-voltage curve. The absolute maximum of the dwell time occurs at the global valley of the current-voltage curve at 0.58 volts; the dwell time subsequently decreases rapidly toward zero (Cf. Ref. [1], Figure 5). The dwell time mimics $1/|j|$, where $j = -enu$ is the current density, since the peak electron density in the well increases monotonically with applied voltage. Microscopic quantum calculations predict that the electron dwell time is maximum at resonance. The QHD model presents a different "macroscopic" interpretation of the dwell time (see the discussion in Ref. [1]).

4. PHASE INFORMATION IN THE QHD MODEL

The computations of multiple resonances and regions of negative differential resistance naturally raise the question: how do the hydrodynamic equations, expressed in terms of macroscopic variables n, $\mathbf{u}$, and T, "know" about quantum interference, which depends on the microscopic phases of the electron wavefunctions? By analyzing the first three moments of the Wigner-Boltzmann equation, I will show how the phases of the electron wavefunctions are present in the hydrodynamic equations.

For a mixed quantum mechanical state described by wavefunctions $\psi_\lambda(\mathbf{x}, t)(\lambda = 1, 2, \ldots)$ with occupation numbers a_λ, the Wigner distribution function is defined as

$$f_W(\mathbf{x}, \mathbf{p}, t) = (\pi\hbar)^{-3}\sum_\lambda a_\lambda \int d^3y \times \psi_\lambda^*(\mathbf{x} + \mathbf{y}, t)\psi_\lambda(\mathbf{x} - \mathbf{y}, t)e^{2i\mathbf{p}\cdot\mathbf{y}/\hbar}. \quad (13)$$

The sum of the occupation numbers $\Sigma_\lambda a_\lambda = M$, where M is the total number of electrons in the system. In general the a_λ's may vary slowly with $\mathbf{x}$ and t. For the purposes of the derivation below, I

will assume the a_λ's are constant. (For a mixed state in thermal equilibrium with a heat bath at temperature $T \equiv 1/\beta$, $a_\lambda \propto e^{-\beta E_\lambda}$.) I will normalize the wavefunctions so that $\int d^3x\, \psi_\lambda^* \psi_\lambda = 1$.

I will assume that the electron flow can be approximated by a single-particle effective mass Schrödinger equation with a self-consistent many-body field:

$$i\hbar \frac{\partial \psi_\lambda}{\partial t} = E_\lambda \psi_\lambda = \frac{\hbar^2}{2m} \nabla^2 \psi_\lambda + V \psi_\lambda \tag{14}$$

where the wavefunctions have energies E_λ and $V(\mathbf{x})$ is the self-consistent potential energy. In the effective mass approximation, Schrödinger's equation with the free electron mass and the total potential energy (the periodic potential energy of the semiconductor lattice plus V) is rewritten with the total potential energy replaced by V and the electron mass replaced by the effective electron mass.

The local average value of an observable χ is defined in the Wigner formalism as

$$\langle \chi(\mathbf{x}, t) \rangle = \int d^3p \chi(\mathbf{x}, \mathbf{p}, t) f_W(\mathbf{x}, \mathbf{p}, t). \tag{15}$$

The first three moments of the Wigner-Boltzmann equation are obtained [8, 1] by setting χ equal to 1, p_j, and $p^2/2m$:

$$\frac{\partial n}{\partial t} + \frac{1}{m} \frac{\partial \langle p_i \rangle}{\partial x_i} = 0 \tag{16}$$

$$\frac{\partial \langle p_j \rangle}{\partial t} + \frac{\partial}{\partial x_i} \left\langle \frac{p_i p_j}{m} \right\rangle = -n \frac{\partial V}{\partial x_j} \tag{17}$$

$$\frac{\partial}{\partial t} \left\langle \frac{p^2}{2m} \right\rangle + \frac{\partial}{\partial x_i} \left\langle \frac{p_i p^2}{2m^2} \right\rangle = -\frac{1}{m} \langle p_i \rangle \frac{\partial V}{\partial x_i} \tag{18}$$

where

$$\langle p_i \rangle = \Pi_i \tag{19}$$

$$\left\langle \frac{p_i p_j}{m} \right\rangle = u_i \Pi_j - P_{ij} \tag{20}$$

$$\left\langle \frac{p^2}{2m} \right\rangle = W \tag{21}$$

$$\left\langle \frac{p_i p^2}{2m^2} \right\rangle = u_i W - u_j P_{ij} + q_i \tag{22}$$

define Π_i, P_{ij}, W, and $\mathbf{q}$. The quantum conservation laws have the same form as their classical counterparts. Explicit factors of $\hbar$ enter only at the fourth and higher moments.

To calculate the average values in the first three moment equations, in Ref. [1] I used the momentum-shifted version of the $O(\hbar^2)$ thermal equilibrium solution [4] to the Wigner-Boltzmann equation. The momentum-shifted $O(\hbar^2)$ f_W need only approximate the actual Wigner distribution function closely enough for the average values in Eqs. (16)–(18) to be close to the actual values. Using this approach, I derived the three-dimensional QHD equations (1)–(3) with Π_i, P_{ij}, and W given by Eqs. (5)–(7).

Since here I am concerned with how phases appear in the QHD equations, I will instead evaluate average values by writing the wavefunction ψ_λ in terms of its magnitude A_λ and phase θ_λ:

$$\psi_\lambda(\mathbf{x}, t) = A_\lambda(\mathbf{x}, t) e^{i\theta_\lambda(\mathbf{x}, t)}. \tag{23}$$

Using this decomposition of the wavefunction, the density is given by

$$\begin{aligned} n &= \int d^3p f_W(\mathbf{x}, \mathbf{p}, t) \\ &= \sum_\lambda a_\lambda \int \frac{d^3p}{(\pi\hbar)^3} d^3y A_\lambda(\mathbf{x} + \mathbf{y}) A_\lambda(\mathbf{x} - \mathbf{y}) \\ &\quad \times e^{-i\theta_\lambda(\mathbf{x}+\mathbf{y}) + i\theta_\lambda(\mathbf{x}-\mathbf{y})} e^{2i\mathbf{p}\cdot\mathbf{y}/\hbar} \\ &= \sum_\lambda a_\lambda A_\lambda^2(\mathbf{x}, t) \equiv \sum_\lambda n_\lambda \end{aligned} \tag{24}$$

where the time-dependence in A_λ and θ_λ is left implicit except when needed for the sake of clarity. n_λ is the electron density for state λ, and the total electron density is obtained by summing over all states. The momentum density equals

$$\begin{aligned} \langle p_i \rangle = \Pi_i &= \int d^3p p_i f_W(\mathbf{x}, \mathbf{p}, t) \\ &= \sum_\lambda a_\lambda \int \frac{d^3p}{(\pi\hbar)^3} d^3y p_i e^{2i\mathbf{p}\cdot\mathbf{y}/\hbar} A_\lambda(\mathbf{x} + \mathbf{y}) \\ &\quad \times A_\lambda(\mathbf{x} - \mathbf{y}) e^{-i\theta_\lambda(\mathbf{x}+\mathbf{y}) + i\theta_\lambda(\mathbf{x}-\mathbf{y})} \\ &= \sum_\lambda a_\lambda \int \frac{d^3p}{(\pi\hbar)^3} d^3y \frac{\hbar}{2i} \left\{ \frac{\partial}{\partial y_i} e^{2i\mathbf{p}\cdot\mathbf{y}/\hbar} \right\} \\ &\quad \times A_\lambda(\mathbf{x} + \mathbf{y}) A_\lambda(\mathbf{x} - \mathbf{y}) e^{-i\theta_\lambda(\mathbf{x}+\mathbf{y}) + i\theta_\lambda(\mathbf{x}-\mathbf{y})} \\ &= -\frac{\hbar}{2i} \sum_\lambda a_\lambda \int \frac{d^3p}{(\pi\hbar)^3} d^3y\, e^{2i\mathbf{p}\cdot\mathbf{y}/\hbar} \\ &\quad \times \frac{\partial}{\partial y_i} \{ A_\lambda(\mathbf{x} + \mathbf{y}) A_\lambda(\mathbf{x} - \mathbf{y}) e^{-i\theta_\lambda(\mathbf{x}+\mathbf{y}) + i\theta_\lambda(\mathbf{x}-\mathbf{y})} \} \\ &= \hbar \sum_\lambda a_\lambda A_\lambda^2(\mathbf{x}, t) \nabla_i \theta_\lambda(\mathbf{x}, t) = \sum_\lambda m n_\lambda u_{\lambda i} \end{aligned} \tag{25}$$

where I have integrated by parts and where the velocity $\mathbf{u}_\lambda$ is defined by

$$\mathbf{u}_\lambda = \frac{\hbar}{m}\nabla\theta_\lambda. \tag{26}$$

This definition agrees with the standard expression for the semiclassical momentum $\mathbf{p}_\lambda = m\mathbf{u}_\lambda = \hbar\nabla\theta_\lambda$ of an electron in state λ. Next I calculate

$$\begin{aligned}\left\langle \frac{p_i p_j}{m} \right\rangle &= u_i \Pi_j - P_{ij} = \int d^3p \frac{p_i p_j}{m} f_W(\mathbf{x}, \mathbf{p}, t) \\ &= -\frac{\hbar^2}{4m}\sum_\lambda a_\lambda \int \frac{d^3p}{(\pi\hbar)^3} d^3y\, e^{2i\mathbf{p}\cdot\mathbf{y}/\hbar} \\ &\quad \times \frac{\partial^2}{\partial y_i \partial y_j}\{A_\lambda(\mathbf{x}+\mathbf{y})A_\lambda(\mathbf{x}-\mathbf{y}) \\ &\qquad \times e^{-i\theta_\lambda(\mathbf{x}+\mathbf{y})+i\theta_\lambda(\mathbf{x}-\mathbf{y})}\} \\ &= \frac{\hbar^2}{2m}\sum_\lambda a_\lambda\big[\{\nabla_i A_\lambda\}\nabla_j A_\lambda - A_\lambda \nabla_i\nabla_j A_\lambda \\ &\qquad + 2A_\lambda^2\{\nabla_i\theta_\lambda\}\nabla_j\theta_\lambda\big] \\ &= \sum_\lambda u_{\lambda i} m n_\lambda u_{\lambda j} - \frac{\hbar^2}{4m}\sum_\lambda n_\lambda \nabla_i\nabla_j \log(n_\lambda).\end{aligned} \tag{27}$$

From Eq. (27), the energy density equals

$$\begin{aligned}\left\langle \frac{p^2}{2m} \right\rangle &= W = \\ &= \frac{\hbar^2}{4m}\sum_\lambda a_\lambda\big[\{\nabla A_\lambda\}^2 - A_\lambda\nabla^2 A_\lambda + 2A_\lambda^2\{\nabla\theta_\lambda\}^2\big] \\ &= \sum_\lambda \frac{1}{2} m n_\lambda u_\lambda^2 - \frac{\hbar^2}{8m}\sum_\lambda n_\lambda \nabla^2 \log(n_\lambda).\end{aligned} \tag{28}$$

Finally

$$\begin{aligned}\left\langle \frac{p_i p^2}{2m^2} \right\rangle &= u_i W - u_j P_{ij} + q_i = \int d^3p \frac{p_i p^2}{2m^2} f_W(\mathbf{x}, \mathbf{p}, t) \\ &= -\frac{i\hbar^3}{16m^2}\sum_\lambda a_\lambda \int \frac{d^3p}{(\pi\hbar)^3} d^3y\, e^{2i\mathbf{p}\cdot\mathbf{y}/\hbar} \\ &\quad \times \frac{\partial^3}{\partial y_i \partial y_j^2}\{A_\lambda(\mathbf{x}+\mathbf{y})A_\lambda(\mathbf{x}-\mathbf{y}) \\ &\qquad \times e^{-i\theta_\lambda(\mathbf{x}+\mathbf{y})+i\theta_\lambda(\mathbf{x}-\mathbf{y})}\} \\ &= \frac{\hbar^3}{8m^2}\sum_\lambda a_\lambda\big[2\big(\{\nabla A_\lambda\}^2 - A_\lambda\nabla^2 A_\lambda\big)\nabla_i\theta_\lambda \\ &\qquad + 4\big(\{\nabla_i A_\lambda\}\nabla A_\lambda - A_\lambda\nabla_i\nabla A_\lambda\big)\cdot\nabla\theta_\lambda \\ &\qquad + A_\lambda^2\big(4\{\nabla\theta_\lambda\}^2\nabla_i\theta_\lambda - \nabla_i\nabla^2\theta_\lambda\big)\big] \\ &= \sum_\lambda u_{\lambda i}\frac{1}{2} m n_\lambda u_\lambda^2 \\ &\quad - \frac{\hbar^2}{8m}\sum_\lambda u_{\lambda i} n_\lambda \nabla^2 \log(n_\lambda) \\ &\quad - \frac{\hbar^2}{4m}\sum_\lambda u_{\lambda j} n_\lambda \nabla_i\nabla_j \log(n_\lambda) \\ &\quad - \frac{\hbar^2}{8m}\sum_\lambda n_\lambda \nabla^2 u_{\lambda i}.\end{aligned} \tag{29}$$

The results in Eqs. (24)–(29) are exact, and do not involve an expansion in $\hbar$. However the moment equations (16)–(18) with expressions (24)–(29) do not form a closed set of equations in terms of hydrodynamic state variables (say n, $\mathbf{u}$ and T or n, Π_i, and W). Note that although the only explicit occurrence of $\hbar$ is $\hbar^2$, the sums over λ will in general involve a functional dependence on $\hbar$.

Spatial derivatives of the wavefunction phases $\theta_\lambda(\mathbf{x}, t)$ appear in the expressions for Π_i, P_{ij}, W, and $\mathbf{q}$ through $\mathbf{u}_\lambda$. Only partial phase information is contained in the first three moment equations, since the fluid dynamical quantities (25) and (27)–(29) involve weighted sums of spatial derivatives of θ_λ.

To make further progress, define

$$\mathbf{u}_\lambda = \mathbf{u} + \tilde{\mathbf{u}}_\lambda \tag{30}$$

where $\mathbf{u}$ is the macroscopic fluid velocity and $\tilde{\mathbf{u}}$ is the velocity with respect to the macroscopic fluid flow. I will assume that the $\tilde{\mathbf{u}}_\lambda$ are random, i.e., that

$$\sum_\lambda n_\lambda \tilde{\mathbf{u}}_\lambda = 0 \tag{31}$$

and that the temperature is defined to leading order by the average of the microscopic kinetic energies of motion relative to the macroscopic fluid flow:

$$\sum_\lambda n_\lambda \frac{1}{2} m \tilde{u}_\lambda^2 = \frac{3}{2} nT + O(\hbar^2). \tag{32}$$

Then I obtain

$$\Pi_i = \sum_\lambda mn_\lambda(u_i + \tilde{u}_{\lambda i}) = mnu_i \tag{33}$$

$$W = \sum_\lambda \frac{1}{2} mn_\lambda(u_i + \tilde{u}_{\lambda i})^2 - \frac{\hbar^2}{8m}\sum_\lambda n_\lambda \nabla^2 \log(n_\lambda)$$

$$= \frac{1}{2}mnu^2 + \frac{3}{2}nT - \frac{\hbar^2}{8m}\sum_\lambda n_\lambda \nabla^2 \log(n_\lambda) + O(\hbar^2) \tag{34}$$

$$P_{ij} = u_i \Pi_j - \sum_\lambda (u_i + \tilde{u}_{\lambda i}) mn_\lambda (u_j + \tilde{u}_{\lambda j})$$

$$+ \frac{\hbar^2}{4m}\sum_\lambda n_\lambda \nabla_i \nabla_j \log(n_\lambda)$$

$$= -\sum_\lambda \tilde{u}_{\lambda i} mn_\lambda \tilde{u}_{\lambda j} + \frac{\hbar^2}{4m}\sum_\lambda n_\lambda \nabla_i \nabla_j \log(n_\lambda)$$

$$= -\delta_{ij} nT + \frac{\hbar^2}{4m}\sum_\lambda n_\lambda \nabla_i \nabla_j \log(n_\lambda) + O(\hbar^2) \tag{35}$$

$$\mathbf{q} = \sum_\lambda \tilde{\mathbf{u}}_\lambda \frac{1}{2} mn_\lambda \tilde{u}_\lambda^2 - \frac{\hbar^2 n}{8m}\nabla^2 \mathbf{u}$$

$$= -\kappa \nabla T - \frac{\hbar^2 n}{8m}\nabla^2 \mathbf{u} + O(\hbar^2). \tag{36}$$

Eq. (35) follows if the Wigner distribution function in the classical limit $\hbar = 0$ is a momentum-shifted Maxwell-Boltzmann distribution (see e.g. Ref. [9], pp. 99–100). In writing the last equation, I have assumed that

$$\sum_\lambda \tilde{\mathbf{u}}_\lambda n_\lambda \nabla^2 \log(n_\lambda) = 0,$$

$$\sum_\lambda \tilde{u}_{\lambda j} n_\lambda \nabla \nabla_j \log(n_\lambda) = 0, \qquad \sum_\lambda n_\lambda \nabla^2 \tilde{\mathbf{u}}_\lambda = 0. \tag{37}$$

The classical heat flux vanishes if the distribution function is a momentum-shifted Maxwell-Boltzmann distribution. The Fourier term $-\kappa \nabla T$ in Eq. (36) is obtained if the Wigner distribution function in the classical limit is the momentum-shifted Maxwell-Boltzmann distribution plus the first-order Chapman-Enskog correction (see Ref. [9], pp. 99–100 and 103–106). Note that I have not used the quantum correction to the heat flux in the simulations presented here.

Even with these simplifications and with $\mathbf{q} = -\kappa \nabla T$, the moment equations (16)–(18) with expressions (24) and (33)–(35) do not form a closed set of equations in terms of hydrodynamic state variables, due to the quantum terms in P_{ij} and W.

The quantum terms in the stress tensor and the energy density were evaluated in Ref. [1] to leading order in $\hbar^2$ by Eqs. (6) and (7). Then the moment equations (16)–(18) do form a closed set in terms of hydrodynamic state variables (say n, $\mathbf{u}$, and T).

The moment equations simplify to a great extent for a pure quantum mechanical state, in which all the a_λ's except one (say a_1) vanish, and $a_1 = 1$. For the pure state,

$$n = A^2 \tag{38}$$

$$\mathbf{u} = \frac{\hbar}{m}\nabla \theta \tag{39}$$

$$P_{ij} = -\frac{\hbar^2}{2m}\left[\{\nabla_i A\}\nabla_j A - A\nabla_i \nabla_j A\right]$$

$$= \frac{\hbar^2 n}{4m}\nabla_i \nabla_j \log(n) \tag{40}$$

$$W = \frac{\hbar^2}{4m}\left[\{\nabla A\}^2 - A\nabla^2 A\right] + \frac{\hbar^2}{2m}A^2\{\nabla\theta\}^2$$

$$= \frac{1}{2}mnu^2 - \frac{\hbar^2 n}{8m}\nabla^2 \log(n) \tag{41}$$

$$\mathbf{q} = -\frac{\hbar^3}{8m^2}A^2 \nabla \nabla^2 \theta = -\frac{\hbar^2 n}{8m}\nabla^2 \mathbf{u}. \tag{42}$$

The expression (42) for $\mathbf{q}$ is written down in Ref. [10], but within a different interpretational framework.

In this case, the moment equations (16)–(18) with expressions (25) and (40)–(42) form a closed set in terms of hydrodynamic state variables n and $\mathbf{u}$. Eqs.

(16)–(18) become

$$\frac{\partial n}{\partial t} + \frac{\partial}{\partial x_i}(nu_i) = 0 \tag{43}$$

$$\frac{\partial}{\partial t}(mnu_j) + \frac{\partial}{\partial x_i}\left(u_i mnu_j - \frac{\hbar^2 n}{4m}\frac{\partial^2}{\partial x_i \partial x_j}\log(n)\right) = -n\frac{\partial V}{\partial x_j} \tag{44}$$

$$\frac{\partial}{\partial t}\left(\frac{1}{2}mnu^2 - \frac{\hbar^2 n}{8m}\nabla^2 \log(n)\right) + \frac{\partial}{\partial x_i}\left[u_i\left(\frac{1}{2}mnu^2 - \frac{\hbar^2 n}{8m}\nabla^2 \log(n)\right) - u_j\left(\frac{\hbar^2 n}{4m}\frac{\partial^2}{\partial x_i \partial x_j}\log(n)\right) - \frac{\hbar^2 n}{8m}\nabla^2 u_i\right] = -nu_i\frac{\partial V}{\partial x_i}. \tag{45}$$

Note that $T = 0$ for the pure state and that the conservation of energy equation (45) follows from the equations for conservation of particles (43) and momentum (44).

For the pure state, then, we have the "hydrodynamic" formulation (see e.g. [11]) of the quantum mechanics of a pure state:

$$\frac{\partial n}{\partial t} + \nabla \cdot (n\mathbf{u}) = 0 \tag{46}$$

$$m\frac{D\mathbf{u}}{Dt} = -\nabla(V + Q) \tag{47}$$

where the advective derivative $D/Dt = \partial/\partial t + \mathbf{u} \cdot \nabla$ and the quantum potential is defined by

$$Q = -\frac{\hbar^2}{2m}\frac{1}{\sqrt{n}}\nabla^2\sqrt{n}. \tag{48}$$

Eqs. (46) and (47) are exact, and follow directly from Schrödinger's equation.

The reader may check that

$$n(x,t) = \begin{cases} C_1 \exp\left(2\sqrt{2m(U - E_\lambda)}\,x\right) & x < -a \\ C_2 \cos^2\left(\sqrt{2mE_\lambda}\,x + \lambda\pi/2\right) & -a < x < a \\ (-1)^\lambda C_1 \exp\left(-2\sqrt{2m(U - E_\lambda)}\,x\right) & x > a \end{cases}$$

$$u(x,t) = 0 \tag{49}$$

is a solution to the "hydrodynamic" equations (46) and (47) for the 1D finite square potential well

$$V(x) = \begin{cases} U & x < -a \\ 0 & -a < x < a \\ U & x > a \end{cases} \tag{50}$$

and reproduces the bound-state solutions for $\psi_\lambda(x,t)$ for $0 < E_\lambda < U$, where $E_\lambda(\lambda = 0, 1, 2, \ldots)$ is the energy of the particle (see e.g. Ref. [12], pp. 152–155). The solution in the square well may be thought of as resulting from the interference of a right moving and a left moving wave. In an analogous but more complicated way, the full quantum hydrodynamic equations "sense" the width of the quantum well in the resonant tunneling diode.

5. CONCLUSION

The macroscopic quantum hydrodynamic equations are capable of modeling effects in quantum semiconductor devices that depend on quantum interference. The interference effects appear in the hydrodynamic expressions for the velocity, stress tensor, energy density, and heat flux through sums involving the semiclassical velocities $\mathbf{u}_\lambda = \hbar\nabla\theta_\lambda/m$.

The QHD simulations of multiple resonances and multiple regions of NDR in the parabolic well resonant tunneling diode clearly demonstrate the effects of quantum interference and present an intuitive macroscopic picture of electron dwell times in the quantum well.

Acknowledgments

I would like to thank Stephen Teitsworth for valuable discussions.

References

[1] C.L. Gardner, "The quantum hydrodynamic model for semiconductor devices," *SIAM Journal on Applied Mathematics*, vol. 54, pp. 409–427, 1994.

[2] M.G. Ancona and G.J. Iafrate, "Quantum correction to the equation of state of an electron gas in a semiconductor," *Physical Review*, vol. B 39, pp. 9536–9540, 1989.

[3] H. Steinrueck and F. Odeh, "The Wigner function for thermal equilibrium," *ZAMP*, vol. 42, 470–487, 1991.

[4] E. Wigner, "On the quantum correction for thermodynamic equilibrium," *Physical Review*, vol. 40, pp. 749–759, 1932.

[5] M.G. Ancona and H.F. Tiersten, "Macroscopic physics of the silicon inversion layer," *Physical Review*, vol. B 35, pp. 7959–7965, 1987.

[6] H.L. Grubin and J.P. Kreskovsky, "Quantum moment balance equations and resonant tunnelling structures," *Solid-State Electronics*, vol. 32, pp. 1071–1075, 1989.

[7] F. Capasso, S. Sen, and F. Beltram, "Quantum-effect devices," in *High-Speed Semiconductor Devices*, pp. 465–520, New York: John Wiley & Sons, 1990.

[8] G.J. Iafrate, H.L. Grubin, and D.K. Ferry, "Utilization of quantum distribution functions for ultra-submicron device transport," *Journal de Physique, Colloque C7,* vol. 42, pp. 307–312, 1981.

[9] K. Huang, *Statistical Mechanics*. New York: John Wiley & Sons, 1963.

[10] S. Sonego, "Interpretation of the hydrodynamical formalism of quantum mechanics," *Foundations of Physics*, vol. 21, pp. 1135–1181, 1991.

[11] C. Philippidis, D. Bohm, and R.D. Kaye, "The Aharonov-Bohm effect and the quantum potential," *Il Nuovo Cimento*, vol. 71 B, pp. 75–88, 1992.

[12] R.B. Leighton, *Principles of Modern Physics*. New York: McGraw-Hill, 1959.

Biographies

CARL L. GARDNER received the B.A. degree in mathematics from Duke University, Durham, NC in 1973, and the Ph.D. degree in physics from MIT, Cambridge, MA in 1981. He is currently Associate Professor of Computer Science and of Mathematics at Duke University. Previously he was Assistant Professor of Computer Science and of Mathematics at Duke University, Associate Research Scientist at the Courant Institute, Assistant Professor of Physics at Bowdoin College, and Instructor of Physics at MIT. His current research interests lie in classical and quantum semiconductor device simulation, and computational fluid and granular dynamics.

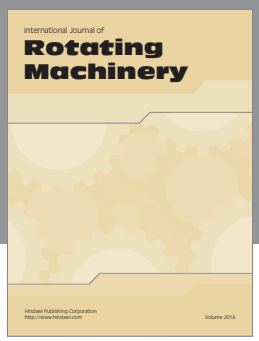

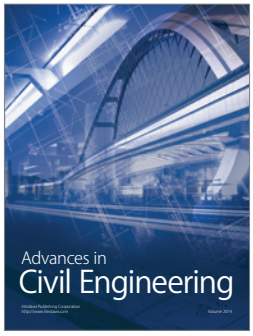

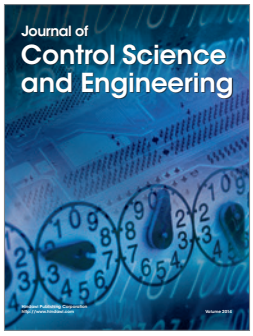

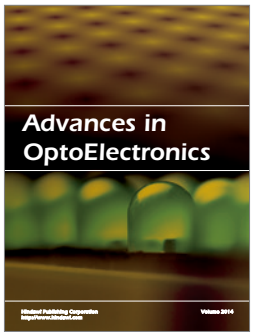

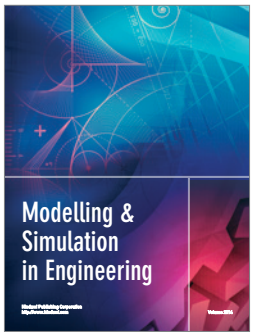

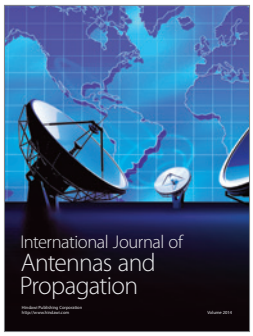

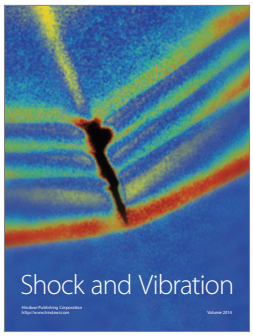

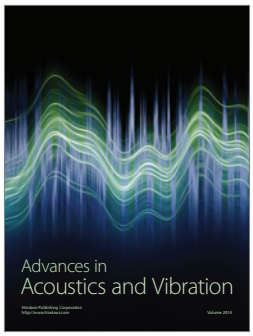

Hindawi

Submit your manuscripts at
http://www.hindawi.com